HHS Public Access

Author manuscript

ACS Nano. Author manuscript; available in PMC 2020 May 28.

Published in final edited form as:

ACS Nano. 2019 May 28; 13(5): 4960–4971. doi:10.1021/acsnano.8b08702.

Dextran-Coated Iron Oxide Nanoparticles as Biomimetic Catalysts for Localized and pH-Activated Biofilm Disruption

Pratap C. Naha[#†,⊗], **Yuan Liu**[#‡,§,⊗], **Geelsu Hwang**[‡,§], **Yue Huang**[†,‡,§], **Sarah Gubara**[†], **Venkata Jonnakuti**[†], **Aurea Simon-Soro**[‡,§], **Dongyeop Kim**[‡,§], **Lizeng Gao**[‖], **Hyun Koo**[*,‡,§], **David P. Cormode**[*,†,⊥,#]

[†]Department of Radiology, University of Pennsylvania, 3400 Spruce Street, 1 Silverstein, Philadelphia, Pennsylvania 19104, United States

[‡]Biofilm Research Laboratories, Levy Center for Oral Health, School of Dental Medicine, University of Pennsylvania, Philadelphia, Pennsylvania 19104, United States

[§]Department of Orthodontics and Divisions of Pediatric Dentistry & Community Oral Health, School of Dental Medicine, University of Pennsylvania, Philadelphia, Pennsylvania 19104, United States

[‖]Institute of Translational Medicine, School of Medicine, Yangzhou University, Yangzhou, Jiangsu 225001, China

[⊥]Department of Bioengineering, University of Pennsylvania, Philadelphia, Pennsylvania 19104, United States

[#]Department of Cardiology, University of Pennsylvania, Philadelphia, Pennsylvania 19104, United States

[#] These authors contributed equally to this work.

Abstract

Biofilms are surface-attached bacterial communities embedded within an extracellular matrix that create localized and protected microenvironments. Acidogenic oral biofilms can demineralize the enamel-apatite on teeth, causing dental caries (tooth decay). Current antimicrobials have low efficacy and do not target the protective matrix and acidic pH within the biofilm. Recently, catalytic nanoparticles were shown to disrupt biofilms but lacked a stabilizing coating required for clinical applications. Here, we report dextran-coated iron oxide nanoparticles termed nanozymes

[*]**Corresponding Authors** Tel: 215-615-4656. Fax: 240-368-8096. david.cormode@uphs.upenn.edu., koohy@upenn.edu.
[⊗]P.C.N. and Y.L. contributed equally to this work.

ASSOCIATED CONTENT

Supporting Information

The Supporting Information is available free of charge on the ACS Publications website at DOI: 10.1021/acsnano.8b08702. Methods for the characterization, stability testing of uncoated NZM, and dextran quantification, zeta potentials of various NZM formulations measured in saliva, biofilm experimental design, effects of different Dex-NZM formulations on bacterial viability and biomass reduction, Dex-NZM iron release assay, TEM of uncoated NZM, stability of Dex-NZM versus uncoated NZM, NZM binding to human cells, effects of uncoated-NZM formulations on cell viability, confocal microscopy images of EPS formation by GtfB, distribution of Dex-NZM within biofilms, confocal microscopy of EPS degradation, investigation of plaque microbiome composition, and optical characterization of Alexa-488 conjugated Dex-NZM (PDF)

The authors declare no competing financial interest.

(Dex-NZM) that display strong catalytic (peroxidase-like) activity at acidic pH values, target biofilms with high specificity, and prevent severe caries without impacting surrounding oral tissues *in vivo.* Nanoparticle formulations were synthesized with dextran coatings (molecular weights from 1.5 to 40 kDa were used), and their catalytic performance and bioactivity were assessed. We found that 10 kDa dextran coating provided maximal catalytic activity, biofilm uptake, and antibiofilm properties. Mechanistic studies indicated that iron oxide cores are the source of catalytic activity, whereas dextran on the nanoparticle surface provided stability without blocking catalysis. Dextran-coating facilitated NZM incorporation into exopolysaccharides (EPS) structure and binding within biofilms, which activated hydrogen peroxide (H_2O_2) for localized bacterial killing and EPS-matrix breakdown. Surprisingly, dextran coating enhanced selectivity toward biofilms while avoiding binding to gingival cells. Furthermore, Dex-NZM/H_2O_2 treatment significantly reduced the onset and severity of caries lesions (vs control or either Dex-NZM or H_2O_2 alone) without adverse effects on gingival tissues or oral microbiota diversity *in vivo*. Therefore, dextran-coated nanozymes have potential as an alternative treatment to control tooth decay and possibly other biofilm-associated diseases.

Graphical Abstract

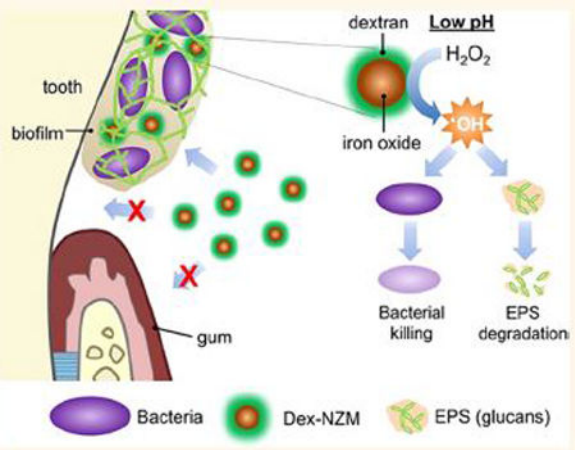

Keywords

nanozyme; biofilm; iron oxide; antibacterial; dental caries

Biofilms are composed of bacterial cell clusters enmeshed within highly structured extracellular matrices of macromolecules such as exopolysaccharides (EPS),[1,2] which provide protection for the resident microorganisms.[2] Many diseases in humans are caused by biofilms, including dental caries (known as tooth decay). Dental caries is a significant threat to public health and is a costly oral infectious disease. More than 30% of children (2–11 years old) and 91% of adults (20–60 years old) are affected by the disease worldwide, with costs for treatment exceeding $120 billion in the US alone.[3–6] Dental caries is a classic biofilm-induced disease that causes the destruction of mineralized tooth tissue and is dependent on the host diet. When dietary sugars are available, oral pathogens such as *Streptococcus mutans* (*S. mutans*), a primary EPS producer and acidogenic bacteria,

assemble an EPS-rich matrix and create a protective and acidic biofilm microenvironment.[7] These adherent and acidic biofilms are difficult to treat and capable of demineralizing the enamel-apatite, leading to the onset of dental caries.[1,8] Conventional antimicrobials, including chlorhexidine, are ineffective in part due to limited efficacy against cariogenic biofilms.[2,9–11] The EPS-rich matrix and the acidic microenvironment created by oral pathogens reduce the antimicrobial activity in the biofilm.[9] Therefore, there is a need for more effective antibiofilm treatments for caries prevention.

Recently, nanotechnology has gained attention for dental applications.[12–19] Zinc oxide[20] and silver[20–23] nanoparticles as well as iron oxide nanozymes (NZM)[12] have been proposed as antibiofilm agents. In particular, uncoated NZM displayed potent antibiofilm actions due to their high peroxidase-like catalytic activity in acidic environments,[12] which can disrupt caries development in the presence of low concentrations of H_2O_2.[12,24] However, for clinical applications, NZM require coatings as uncoated nanoparticles lack stability in physiological media and in solutions suitable for therapeutic formulations and can bind to biological tissues indiscriminately, which could lead to adverse effects to healthy tissues.[25,26] Ideally, the presence of coatings would improve biofilm targeting and maintain catalytic activity, while enhancing biocompatibility, which could result in a more practical and specific antibiofilm treatment.

Dextran is a polysaccharide derived from microorganisms and, when added to a growing biofilm, can be incorporated into the matrix by bacterial exoenzymes (*e.g., S. mutans*-derived glucosyltransferases) that use dextran as an acceptor molecule to synthesize EPS glucans.[27,28] Importantly, dextran is a FDA-approved polymer, and dextran-coated iron oxide nanoparticles, such as Feridex, have been FDA approved for systemic use as MRI contrast agents.[29] Therefore, we hypothesized that dextran-coated NZM (Dex-NZM) could be incorporated into biofilms while maintaining its intrinsic catalytic activity to break down the EPS structure and kill bacteria upon exposure to H_2O_2 at cariogenic (acidic) pH values. In addition, dextran coating would also result in stability in aqueous formulations and provide biocompatibility to the host soft tissue in the oral cavity. Here, we have developed Dex-NZM using dextran with a range of molecular weights (from 1.5 kDa to 40 kDa). We examined their catalytic properties, cytotoxicity, biofilm uptake, and antibiofilm activity to determine optimal coating characteristics. For a selected, mostly bioactive formulation (10 kDa), we probed its catalytic activity, biofilm targeting, and cellular interactions in detail using spectroscopic and high-resolution imaging with biochemical methods. Furthermore, the selected Dex-NZM was tested for its efficacy to control the onset and severity of dental caries using a rodent model of the disease. Histological and microbiome analyses were performed on the soft-tissues, oral microbiota diversity, and composition to confirm the safety of the agent.

RESULTS AND DISCUSSION

In this study, we developed Dex-NZM for the treatment of biofilms associated with dental caries. Since Feridex is FDA-approved and has been used for tumor and atherosclerotic plaque imaging,[29,30] we hypothesized that the presence of a dextran coating on the nanoparticle surface could enhance biofilm targeting specificity and biocompatibility

without significantly impacting the catalytic activity of the iron oxide core.[31–33] We tested several different formulations that were synthesized using different dextran molecular weights and found that 10 kDa dextran-coated NZM provided an optimal balance of catalytic activity, biofilm uptake, and when exposed to low H_2O_2 concentration, resulted in marked bacterial killing and biofilm reduction, preventing caries severity without adverse effects *in vivo.*

Dextran-Coated NZM Maintain Catalytic Activity.

Dex-NZM formulations were synthesized using a range of dextran molecular weights since we sought to understand the effect of the molecular weight of the coating on catalytic activity, biofilm incorporation, and antibiofilm effects. TEM of Dex-NZM formulations (Figure 1A) revealed that nanoparticles were formed in each case. The core sizes of Dex-NZM coated with 1.5, 5, 10, 25, and 40 kDa dextran are 32.5 ± 14.2, 14.7 ± 3, 11.4 ± 1.8, 15.6 ± 3.6, and 32.2 ± 9.6 nm, respectively. The iron oxide cores formed with 5, 10, and 25 kDa dextran were similar in morphology, whereas very heterogeneous iron oxide cores were formed when 1.5 and 40 kDa dextran was used. Seemingly 5–25 kDa is a range in which the dextran molecular weight is better suited for iron oxide core nucleation. The hydrodynamic diameters of these Dex-NZM formulations range from 30 to 60 nm, without a clear correlation with dextran molecular weight (Figure 1B). Unsurprisingly, their zeta potentials were similar, all being slightly negative, consistent with other reports for dextran-coated iron oxide nanoparticles (Figure 1B and Table S1).[34] The peroxidase-like activities of Dex-NZM were measured using the colorimetric TMB (3,3',5,5'-tetramethylbenzidine) assay. This assay is a well-established method for peroxidase-like activity determination, where optical absorbance can be used to measure the oxidation of the TMB substrate by hydrogen peroxide and the catalyst.[32,35] These experiments were done at pH 4.5, 5.5, and 6.5 to span the range of pHs expected to exert catalytic activity. Stronger catalytic activities were observed at more acidic pH, *i.e.,* 4.5 (found in cariogenic biofilms[1,8]) compared to pH 6.5 (noncariogenic) for all formulations, indicating that damage caused by reduction of hydrogen peroxide and consequent generation of reactive oxygen species would be higher against pathological biofilms (Figure 1C). Interestingly, the highest catalytic activity was observed for the 10 kDa dextran formulation, which is likely due to its smallest core size, resulting in the highest surface area.

Dex-NZM Incorporation into Biofilms and Bioactivity Assessment.

To determine whether Dex-NZM were taken up in biofilms, we performed topical treatments using an established saliva-coated hydroxyapatite (pellicle-coated tooth mimetics) biofilm model under cariogenic conditions using the oral pathogen *S. mutans* grown in the presence of sucrose (Figure S1). We found that these nanoparticles were retained within biofilms when applied topically and that 10 kDa Dex-NZM was taken up to the greatest extent as determined by ICP-OES (Figure 2A). The bioactivity of Dex-NZM formulations in terms of bacterial killing and biomass reduction efficacy were assessed with *S. mutans* biofilms with or without H_2O_2 exposure. A significantly greater bactericidal effect was observed with all Dex-NZM/H_2O_2 compared to H_2O_2 alone or control (Figure 2B). When treated with Dex-NZM alone (without H_2O_2), some antibacterial activity was observed (Figure S2A), although to a much lesser extent than for the combination of Dex-NZM and H_2O_2. The

bactericidal effects of the 1.5, 5, and 10 kDa dextran formulations were similar, reducing the number of viable bacteria by 6-log colony forming units (CFU). On the other hand, 25 and 40 kDa dextran formulations were less effective, albeit still capable of reducing bacterial viability by 4–5 log CFU. Furthermore, biofilm biomass disruption is an important parameter for determining antibiofilm efficacy.[17] The 10, 25, and 40 kDa dextran formulations reduced bacterial biomass (dry weight) significantly more than H_2O_2 alone (Figure 2C). However, we did not observe significant biomass reductions with the 1.5 and 5 kDa dextran formulations compared with H_2O_2 alone (Figure 2C). Interestingly, a similar biomass reduction effect was observed for Dex-NZM incubations, regardless of H_2O_2 (Figure S2B).

Next, the biocompatibilities of Dex-NZM formulations were tested with human primary oral gingival cells and human fibroblast cells. We found that none of the Dex-NZM formulations inhibited the viability of either cell type when incubated at a concentration of 0.5 mg of iron/mL (Figure 2D,E). When selecting which formulation to pursue for further in-depth studies, *i.e.*, analysis of catalytic activity, binding specificity, imaging of bacterial killing, EPS degradation *in situ*, and *in vivo* testing, we focused on antibacterial activity and biomass reduction. We chose the 10 kDa dextran formulation since it was the only one that had both high bacterial killing and significant biomass disruption. Moreover, the FDA-approved dextran coated iron oxide nanoparticle uses 10 kDa dextran,[29] further motivating more detailed study of this formulation and its use for *in vivo* efficacy evaluation.

Dextran Coating Influences on Catalytic Activity, Stability, and NZM Biofilm Binding.

To further understand the behavior of Dex-NZM, we performed additional studies to assess catalytic performance and bioactivity in detail, including the role of dextran (vs uncoated NZM) and biofilm uptake and incorporation into biofilm structure *via* EPS. The catalytic reaction mechanism was explored by evaluating its kinetics with the TMB assay under different reagent concentrations, using horseradish peroxidase (HRP) as a control. The data were a good fit for the Michaelis-Menten equation, which permitted the derivation of the reaction constants (K_m). The K_m values for H_2O_2 were found to be 27 μM and 2.5 mM for Dex-NZM and HRP, respectively (Figure 3A). The data revealed that this Dex-NZM formulation has high affinity for the hydrogen peroxide substrate as indicated by lower K_m values.[35]

Our data show that Dex-NZM has high catalytic activity in acidic environments. However, IONP can release iron ions in such acidic environments.[12,36] Therefore, we sought to determine whether these released ions could contribute to the catalytic activity *via* the Fenton reaction. To answer this question, we performed iron ion release experiments at pH 4.5 and determined the catalytic activity of the released iron ions (Figure S3A and B). Low percentages of the iron ions were released and the released iron ions account for a relatively small fraction of the overall catalytic activity. Therefore, the iron cores themselves were the main contributor of the catalytic activity. In addition, we examined the role of the dextran coating on catalytic activity. We compared the catalytic activity of Dex-NZM and uncoated NZM (Figure S4) of similar core size to Dex-NZM and found that the dextran coating reduced activity somewhat, in line with results found by others[31] (Figure 3B). Furthermore,

the activity of dextran alone was very low, and when dextran was mixed with uncoated NZM at the concentration found in Dex-NZM (5.4:1 dextran to iron mass ratio), there was not a statistically significant difference in activity compared with uncoated NZM alone. Therefore, dextran coatings do not contribute to catalytic activity, but allow reagents to access iron oxide cores so that catalytic activity occurs. Furthermore, we found that Dex-NZM was catalytically active within a cariogenic biofilm (Figure 3C).

Given that dextran coating could enhance dispersibility and exogenous dextran can be incorporated into EPS matrix,[27,28,37] we hypothesized that Dex-NZM could display improved formulation stability and binding specificity toward biofilms rather than mammalian tissues or uncolonized tooth surfaces. In order to probe this question, we used the aforementioned uncoated NZM as a comparator. The Dex-NZM was stable and did not settle in any of the media tested, underscoring the potential clinical utility and commercial potential of this agent (settling in storage could result in uneven dosing to the subject). We found that Dex-NZM is well suspended in water, PBS, and saliva (Figure 3D and S5), but uncoated NZM are not stable in PBS and saliva as evidenced by settling to the bottom of the vial when suspended in PBS or saliva (at 1 h) and even in DI water (at 24 h). Next, we tested the selectivity of uncoated and dextran-coated NZM. Excitingly, we found that Dex-NZM was unable to bind to mammalian cells (both oral gingival and fibroblast cells), whereas uncoated NZM bound very strongly and in high amounts, as evidenced by ICP-OES measurements (Figure 3E), and could also be observed by visual inspection of the cells (Figure S6). On the other hand, Dex-NZM and uncoated NZM were both taken up in biofilms significantly (Figure 3F). We also examined the effect of uncoated NZM binding to mammalian cells by assessing the viability of human gingival epithelial cells. We found that uncoated NZM resulted in significant reductions in cell viability at 24 h (Figure S7), which emphasized the adverse effects of their nonspecificity.

We further examined the uptake of these nanoparticles in biofilms by testing their incorporation into EPS formed on hydroxyapatite surfaces *via* the action of GftB. Dex-NZM were incorporated into EPS to a much greater extent than uncoated NZM (Figure 3G), likely due to Dex-NZM's chemical similarity to dextran, which can be incorporated into the EPS structure during glucan synthesis by *S. mutans*-derived GtfB exoenzymes *via* acceptor reaction.[38] This result was supported by confocal microscopy of glucans formed by GtfB in the presence of Alexa-488 labeled Dex-NZM, where we observed strong colocalization of the EPS and Dex-NZM fluorescence (Figure S8). Moreover, we examined the binding of these nanoparticles to saliva coated hydroxyapatite (sHA) as a tooth surface mimetic and observed that Dex-NZM had much lower binding to the apatitic surface than uncoated NZM (Figure 3H). Thus, we unexpectedly found that while Dex-NZM were taken up by biofilms, they were unable to bind to mammalian cells and less avidly to sHA, while uncoated iron oxides were bound to all tested surfaces, highlighting the selectivity of Dex-NZM toward biofilms.

Bacterial Killing and EPS Degradation within Bio-films.

To further assess the Dex-NZM binding and antibiofilm activity, we employed high-resolution confocal fluorescence imaging combined with quantitative computational

analysis. Alexa-488 conjugated Dex-NZM was employed to visualize the nanoparticle distribution within biofilm architecture. Representative confocal images show Dex-NZM (labeled in green) associated with the entire bacterial cluster (in gray) and also incorporated throughout the EPS matrix (in purple) structure (Figure 4A-D). We found that approximately 49% of Dex-NZM were colocalized with bacteria and 51% with the EPS. In addition, we found that Dex-NZM penetrated into the biofilm (up to 40 μm penetration vs 56 μm average biofilm height) with a fairly even distribution (Figure S9). We next examined localized bacterial killing and EPS breakdown on selected areas (white and yellow squares; Figure 4E). Under addition of H_2O_2, the numbers of dead bacteria (in red) markedly increased (Figure 4F,H), and concurrently, the EPS matrix (in purple) was degraded (Figure 4G,I), indicating antibiofilm effects *in situ via* the catalytic activity of Dex-NZM. The antibacterial and EPS degradation activities of Dex-NZM/H_2O_2 were confirmed as determined by fluorescence intensity changes over time (Figure 4J,K), consistent with microbiological and biomass data (Figure 2B,C) and confocal imaging (Figure 4F,H/G,I). Peroxidase-like activity can result in the production of free radicals, which can kill bacterial cell and degrade the EPS, as noted by others.[39,40] Moreover, we studied the effects of Dex-NZM on EPS alone using a time- lapsed confocal microscopy experiment (Figure S10) and found that only the combination of Dex-NZM and hydrogen peroxide resulted in significant degradation of the EPS. Given our positive results using Dex-NZM as an antibiofilm agent, it is conceivable that a peroxidase conjugated to dextran might also prove to be efficacious and would be interesting to test. However, Dex-NZM will likely have advantages over such a construct, being lower cost and easier to mass produce, possessing longer lasting activity as natural enzymes suffer from proteolytic degradation in biological settings and avoiding issues of immunogenicity.[31,47,48] Furthermore, we tested the antibiofilm activity of horseradish peroxidase combined with hydrogen peroxide and found it to minimally improve bacterial killing (data not shown), compared with hydrogen peroxide alone.[49]

Altogether, the *in vitro* data demonstrate biofilm targeting specificity by Dex-NZM, which in turn can effectively kill bacterial cells and degrade EPS matrix in pathogenic acidic biofilms when activated by H_2O_2. These results indicated that Dex-NZM, when used as a topical oral treatment, would be selective for biofilms over the host tissues in the oral cavity, impacting caries development while sparing mammalian host cells *in vivo*.

Dex-NZM Suppress Biofilm Associated Dental Caries *in Vivo*.

The *in vivo* efficacy of Dex-NZM as an anticaries treatment was evaluated in a well-established rodent model of dental caries.[41] In addition to mineralized tooth tissue, both the effects on soft tissue and on the oral microbiota composition/diversity were examined. In this model, tooth enamel progressively develops caries lesions (analogous to those observed in humans), proceeding from initial areas of demineralization to moderate lesions and on to extensive (severe) lesions characterized by enamel structure damage and cavitation. We simulated the treatment conditions that might be experienced clinically in humans by applying the test agent solutions topically twice daily with a brief, 1 min exposure time. We found that Dex-NZM/H_2O_2 treatment was highly effective in reducing caries development in both smooth and sulcal surfaces (Figure 5A and B), resulting in significantly less overall caries lesions compared to vehicle control and Dex-NZM or H_2O_2 alone. Importantly, the

severity of caries lesions was progressively blocked and completely prevented extensive lesions and cavitation on smooth dental surface. Furthermore, the efficacy of Dex-NZM/H_2O_2 was significantly higher than H_2O_2 or Dex-NZM alone (Figure 5A,B), supporting the catalytic–therapeutic mechanism of Dex-NZM/H_2O_2 *via* its intrinsic catalytic activity.

In vivo data provided further validation of biocompatibility after 21 days of topical treatment *via* analysis conducted on the gingival tissues and the oral microbiota. Histopathological analysis on gingival tissues revealed no visible signs of adverse effects, such as proliferative changes, inflammatory responses, or necrosis, of treatment with Dex-NZM, or H_2O_2 or the Dex-NZM/H_2O_2 (Figure 5C). This result supports our *in vitro* findings showing that Dex-NZM lacks cytotoxic effects and more selectively binds to bacterial biofilms rather than gingival epithelial cells. The effects of Dex-NZM/H_2O_2 on oral microbiota were also evaluated, and no statistically significant changes of oral microbial composition and diversity were found between the treatment groups (Figure S11). Therefore, our treatment strategy did not disrupt the ecological balance of the oral microbiota and did not adversely affect the adjacent tissues in the oral cavity, while being highly effective in reducing dental caries. The lack of effect on the oral microbial composition is likely because the Dex-NZM have increased catalytic and bactericidal activity at low pH values found in cariogenic biofilms arising from acidogenic bacteria such as *S. mutans.* These *in vivo* results support our *in vitro* data of specificity against acidic biofilms.

The observation of catalytic activity arising from coated iron oxide nanoparticles is also important. Surface coating of nanozymes can affect their enzyme-like activity, since binding of the coating to the nanoparticle reduces the surface available to interact with substrates.[31,45] In biological applications of nanozymes, it is often necessary to find coatings that provide both stability in physiological fluids as well as allow access of substrates to the nanoparticle surface.[15]

We found that dextran coating did not silence the peroxidase-like activity of iron oxide nanoparticles. This finding agrees with a previous report,[31] although the iron oxide nanoparticles were more than 10-fold larger than in this study. It also agrees with previous reports of dextran coating of iron oxide nanoparticles leaving gaps on their surfaces.[46] This property may play a role in other bioactivities that have been observed to arise from iron oxide nanoparticles.[42,43] It may be the case that this catalytic activity could be used against biofilms in other settings such as joint replacements or catheters. The efficacy of the Dex-NZM/H_2O_2 combination may indicate that other peroxidase mimics, such as graphene,[35] will have similar antibiofilm effects. In addition, the biofilm targeting effect that we found with dextran could potentially be used with other materials such as gold nanoparticles.[44] The advantages of Dex-NZM are further highlighted by their comparison with uncoated NZM. We found that uncoated NZM bind indiscriminately to biofilms and tissues in the mouth (i.e., they bound to mammalian cells and hydroxyapatite), whereas Dex-NZM bound selectively to biofilms. Moreover, we found that Dex-NZM were well suspended in different solutions tested, while the uncoated NZM settled rapidly in each fluid. The settling of a formulation is a significant drawback for practical consumer product development since the

dose might be dispensed unevenly, leading to reduced effectiveness in addition to possible adverse effects due to unspecific binding.

Dex-NZM might have applications for other oral diseases and against additional bacterial strains; however, this technology may have limitations when the local pH environment is not acidic (e.g., periodontal diseases) or with microoganisms that can degrade H_2O_2. Another potential drawback is the possibility of iron staining of enamel. We found that Dex-NZM to bound poorly to saliva-coated hydroxyapatite *in vitro* (Figure 3H) and minimally leached free irons even at acidic pH, and we did not observe any discoloration over the 21 day period of the *in vivo* experiment. Nevertheless, more extensive testing will be required to establish that Dex-NZM does not stain teeth in humans. Lastly, lack of visualization of biofilms on the teeth from the animal experiments and unavailability of appropriate uncoated NZM control due its aforementioned issues are experimental limitations of this study. Further detailed analysis of the *in vivo* biofilms following treatment and inclusion of NZM control with inert nondextran coatings in addition to dosage and treatment duration optimization shall reveal important mechanistic insights as well as advance this catalytic nano-therapeutic approach.

In summary, Dex-NZM is very stable in saliva or physiological buffers, biocompatible, does not bind to mammalian cells, is retained within bacterial biofilms, and is effective in reducing dental caries. In addition, Dex-NZM/H_2O_2 does not adversely affect oral microbiota diversity and composition. The translation of this treatment to use in humans is likely practical, since the costs of the various reagents, such as iron salts and hydrogen peroxide, are quite low and readily available. The treatment could be supplied as a mouthwash with a bottle containing two chambers or in toothpaste form where the nanoparticles and hydrogen peroxide are kept separate until the toothpaste is dispensed. It might be possible to develop a formulation that self- generates hydrogen peroxide, thereby circumventing the need for two chambers in the container, although such an agent may be more complex and expensive. Additional dosing and safety studies would have to be done before testing in humans; however, the prior FDA-approval of similar iron oxide nanoparticles for systemic use (at several hundred-fold higher dosage) and the limited exposure received *via* topical applications in the oral cavity provide reasons to be optimistic about the safety of this approach. We also envision this therapeutic approach to be particularly useful for patients with or at high risk of developing severe childhood caries, an aggressive form of disease characterized by rampant tooth decay, that is often associated with iron deficiency.

CONCLUSIONS

We report herein that dextran-coated iron oxide nanozymes are an effective antibiofilm agent for an oral disease. Despite the dextran coating, these nanozymes possess peroxidase-like catalytic activity and have additional attractive attributes such as stability and targeting specificity. Dex-NZM display peroxidase-like activity at pathological acidic pH values, efficiently target biofilm cells, and degrade EPS matrix *via* catalytic activation of H_2O_2. Further analyses revealed that the catalytic activity arises from the iron cores of these nanoparticles and that their dextran coating provides selective binding to bacterial cells over

oral epithelial cells while facilitating incorporation into biofilm matrix. *In vivo* results showed that Dex-NZM mediated H_2O_2 catalysis potently disrupted the onset of a costly and highly prevalent oral biofilm-associated infection (dental caries or tooth decay). The nanozyme-based topical therapy markedly reduced the number and severity of caries lesions compared to controls. Histological and microbiome analyses revealed no adverse effects on the surrounding host tissues and oral microbiota diversity *in vivo*, consistent with lack of cytotoxicity and biofilm-targeting specificity observed *in vitro.* Altogether, Dex-NZM is a potent and biocompatible antibiofilm agent. There are limitations of this technology, such as when the local pH environment is not acidic or against bacterial strains that can degrade H_2O_2, while the potential of tooth staining and in-depth safety studies need to be conducted and assessed. Nevertheless, given the prior FDA-approval of similar agents, this nanozyme-based approach could provide an excellent therapeutic platform for alternative product development to prevent the burdensome disease of dental caries. At the same time, the availability and low cost of the materials and chemical flexibility of iron oxide nanoparticles could galvanize a wider investigation of this approach for clinical applications to treat other biofilm-related maladies.

MATERIALS AND METHODS

Synthesis of Dextran-Coated NZM (Dex-NZM).

A range of Dex-NZM formulations were synthesized based on a protocol published elsewhere,[36] using varying dextran molecular weights (from 1.5 to 40 kDa). In brief, 12.5 g of dextran (Pharmacosmos, Holbaek, Denmark) of the selected molecular weight was dissolved in 25 mL of deionized (DI) water. Once the dextran completely dissolved in DI water, the solution was placed in an ice bath and purged with nitrogen gas to remove oxygen from the flask. A 0.985 g portion of ferric chloride hexahydrate and 0.366 g of ferrous chloride tetrahydrate (Sigma-Aldrich, St. Louis, MO) were each dissolved in 6.25 mL of DI water separately and then added to the dextran solution. The reaction mixture was allowed to stir for 45 min at 4 °C for complete mixing of iron salts with dextran solution.

Next, 15 mL of ammonium hydroxide (28–30%, Sigma-Aldrich) was added to the reaction mixture using a syringe pump. The ammonium hydroxide was added to the reaction mixture at different rates, i.e., 0.3 μL/min for the first 2.5 h and then 0.6, 0.9, and 1.2 μL/min for 1 h each consecutively. The remainder of the ammonium hydroxide was added to the reaction mixture at a rate of 4 μL/min. After the addition of ammonium hydroxide was completed, the reaction mixture was heated to 90 °C for 1 h and then stirred overnight at room temperature. The nanoparticle suspension was then spun at 20000 rcf for 30 min at 4 °C, after which the supernatant was collected and concentrated using ultrafiltration tubes (molecular weight cut off 100 kDa, Sartorius Stedim Biotech, Germany). The concentrated Dex-NZM was purified with citrate buffer *via* diafiltration columns (100 kDa, Spectrum Labs, CA). After purification, Dex-NZM was stored at 4 °C. Conjugation with Alexa 488 NHS Ester (ThermoFisher Scientific) was achieved by introducing amine groups to the dextran coating, as previously described, and then following the manufacturer's instructions. These fluorescent nanoparticles were further purified using ultrafiltration tubes (molecular weight cut off 100 kDa, Sartorius Stedim Biotech). UV—vis (Evolution 201 UV—vis

spectrophotometer, ThermoFisher Scientific) and fluorescence spectra (SpectraMax, M5, Molecular Devices) proved that Alexa-488 was conjugated successfully to the nanoparticle surface (Figure S12). Uncoated NZM were synthesized by first dissolving 1.1 g of ferric chloride hexahydrate and 0.4 g of ferrous chloride tetrahydrate (Sigma-Aldrich) in 15 mL of DI water each and then transferring these solutions to a three-necked flask. The reaction mixture was stirred under an inert nitrogen atmosphere. The reaction mixture was heated to 85 °C, and then 20 mL of diluted ammonium hydroxide solution (2.5 mL of 28% ammonium hydroxide diluted to 20 mL with DI water) was added dropwise to the reaction mixture. After addition of ammonium hydroxide, the reaction mixture was stirred at 85 °C for 1 h. Next, the nanoparticles were collected magnetically and were purified with DI water using diafiltration columns (100 kDa).[51]

Characterization of Dex-NZM.

Hydrodynamic Diameter and Zeta Potential.—The hydrodynamic diameter and zeta potential of each Dex-NZM were measured using a Nano-ZS 90 (Malvern Instrument, Malvern, UK). Then 1.5 and 1 mL of diluted Dex-NZM (12.5 μL Dex-NZM stock solution to 1 mL of DI water) were used for the hydrodynamic diameter and zeta potential measurements, respectively.

Transmission Electron Microscopy.—Transmission electron microscopy (TEM) of each Dex-NZM was performed using a JEOL 1010 microscope operating at 80 kV. Then 5 μL of nanoparticle suspension was dropped onto the TEM grid (FCF-200-Cu, Electron Microscopy Sciences, Hatfield, PA), and the liquid was allowed to dry before microscopy was performed.

Inductively Coupled Plasma Optical Emission Spectroscopy.—The iron concentration in each Dex-NZM formulation was measured using inductively coupled plasma optical emission spectroscopy (ICP-OES).[52] Then 5, 10, or 25 μL of Dex-NZM was dissolved in 1 mL of aqua regia. After complete dissolution of Dex-NZM, the final volume in each tube was adjusted to 10 mL with DI water. The iron concentration was measured using ICP-OES (Spectro Genesis ICP). The concentration obtained from the ICP-OES was adjusted by the dilution factor for each sample and then averaged to determine the iron concentration in the stock solution.

The total amount of iron within intact biofilms (*i.e.*, bacterial cells and EPS combined) was also measured using ICP-OES. Biofilms treated with Dex-NZM formulations were transferred to glass tubes and digested with 1 mL of aqua regia overnight at room temperature. Then the volume was adjusted to 10 mL with DI water prior to analysis with ICP-OES. Three independent experiments were performed for each Dex-NZM formulation, and the data are presented as mean ± SD.

Catalytic Activity (TMB) Assay.—The peroxidase-like catalytic activities of the Dex-NZM formulations were investigated *via* a colorimetric assay using 3,3',5,5'-tetramethylbenzidine (TMB, Sigma-Aldrich) and hydrogen peroxide (H_2O_2) following a previously published protocol, with a slight modification. This assay is well-established as

an assessment of peroxidase-like activity,[32,35] where hydrogen peroxide and the TMB substrate are converted to water and an oxidized form of TMB that is blue in color. UV/vis measurements at 652 nm allow the oxidation of TMB to be monitored and catalytic activity to be compared. The catalytic activity of each Dex-NZM was measured at three different pH values, *i.e.*, 4.5, 5.5, and 6.5. The assay was performed in 96-well plates. A 300 μL portion of 0.1 M sodium acetate (NaAc) buffer at the appropriate pH was added to each well of a 96-well plate. Then, 1.2 μL of Dex-NZM (5 mg Fe/mL) was added to the wells. After the addition of Dex-NZM, 3 μL TMB (10 mg/mL) and 15 μL of H_2O_2 (0.5% v/v) were added to each well and mixed vigorously. After addition of hydrogen peroxide, the 96 well plate was immediately placed into a plate reader, and the absorbance was recorded at 652 nm at 1 min intervals for 30 min. Three independent experiments were performed for each Dex-NZM formulation. The slope of the line was calculated and averaged, and the data are presented as mean ± SD.

Kinetics of Peroxidase-like Activity.—The reaction kinetic assay was carried out using a UV-vis spectrophotometer (Beckman Coulter DU 800). These experiments are based on the same reaction as above, but varying the reaction conditions allows more detailed catalytic parameters to be derived. Briefly, 10 μL of 2 mg/mL of Dex-NZM and 10 μL of 10 mg/mL TMB were added to several NaAc buffer samples (970 μL, pH 4.5). Next, 10 μL of different concentrations of H_2O_2 (*i.e.*, 2.5, 5, 10, 25, 50, 75 mM) were added to the above solutions and mixed *via* pipetting. The absorbance of all samples was recorded at 652 nm immediately after addition of H_2O_2. For the TMB reaction kinetics, 10 μL of different concentrations of TMB stock solution (i.e., 2, 5, 10, 20, 50 mg/mL) and 10 μL of H_2O_2 (0.5%, w/w) were used for determination of the K_m value. Absorption data were used to calculate the concentration of the TMB oxidation product using the Beer-Lambert law using a molar absorption coefficient of 39000 M^{-1} cm^{-1} . The reaction velocity was measured based on the slope of the absorption versus time curve during the first 5 min.

Iron Release and Catalytic Activity of Released Iron Ions.—The effect of iron ion release from 10 kDa Dex-NZM was studied in 0.1 M NaAc buffer (pH 4.5). A 1 mL portion of Dex-NZM (5 mg Fe/ml) was diluted with 9 mL of 0.1 M NaAc buffer. After mixing, samples were incubated at 37 °C for 5, 30, 60, and 120 min (n = 3 per time point). After the desired incubation time, the free iron ions and nanoparticles were separated using ultrafiltration tubes (10 kDa MWCO). The iron content in the filtrate and the nanoparticle pellet from each incubation time point were measured using ICP-OES. The catalytic activity of the released iron in the supernatant and nanoparticle pellet from each incubation time point was analyzed using the TMB assay, as described above. Three independent experiments were performed per incubation time point, and the data are presented as mean ± SD.

Dex-NZM Incorporation into EPS by Glucosyltransferase B (GtfB).—To assess the incorporation of Dex-NZM into EPS, the purified GtfB enzyme was adsorbed on hydroxyapatite (HA) beads (Macro-Prep Ceramic Hydroxyapatite Type 1, 80 μm, Bio-Rad), which had been coated with clarified whole saliva as described previously.[53] Following adsorption of GtfB, the beads were washed three times with adsorption buffer and exposed

to Dex-NZM in sucrose substrate at a concentration of 0.5 mg/mL for 4 h with rocking at 37 °C. The amounts of Dex-NZM incorporated into glucans were determined by ICP-OES. Moreover, EPS glucans were produced by purified *S. mutans*-derived GtfB immobilized on poly-L-lysine coated MatTek dishes and incubated with 0.25 mg/mL of Alexa Fluor 488 labeled Dex-NZM for 2 h. Then confocal imaging (Zeiss LSM 800 upright laser scanning microscope) was performed using a 20× (numerical aperture = 1.0) water immersion objective. The glucans were visualized by inherent reflection optical property using a 405 nm laser and a 445/50 nm emission filter. Dex-NZM were imaged using 488 nm excitation and a 520/40 nm emission filter.

Dex-NZM Binding to Saliva-Coated Hydroxyapatite Beads.—In this binding assay, 10 mg of saliva-coated HA beads was incubated in 500 μL of Dex-NZM solution at a concentration of 0.2 mg/mL for 30 min with rocking at 37 °C. Then the supernatant was removed, and the beads were washed three times with water to remove unbound nanoparticles. The beads were dissolved with 1 mL of 70% HNO_3, and the iron was analyzed *via* ICP-OES.

Oral Biofilm Model.—Biofilms were formed on saliva-coated hydroxyapatite (sHA) disks (surface area, 2.7 ± 0.2 cm^2, Clarkson Chromatography Products Inc., South Williamsport, PA), as described elsewhere,[38,54] that were vertically suspended in 24-well plates. *Streptococcus mutans* UA159 (ATCC 700610) was grown in . ultrafiltered (10 kDa molecular-mass cutoff) tryptone-yeast extract broth (UFTYE; 2.5% tryptone and 1.5% yeast extract) containing 1% (wt/vol) glucose at 37 °C and 5% CO_2 to midexponential phase. Each HA disk was coated with filter-sterilized saliva for 1 h at 37 °C (the saliva was prepared as described previously).[38,54] These sHA disks were each inoculated with ~2×10^5 colony forming units (CFU) of *S. mutans* per milliliter in UFTYE culture medium (pH 7.0) containing 1% (wt/vol) sucrose at 37 °C. The culture medium was changed twice daily (at 19 and 29 h) until the end of the experimental period (43 h). The biofilms were collected and analyzed for Dex-NZM binding and catalytic activity as well as bioactivity as described below.

Bacterial Killing and Biomass Reduction by Dex-NZM with H_2O_2.—To assess the antibiofilm effect of Dex-NZM bound within biofilms, the sHA disks and biofilms were topically treated twice daily by placing them in 2.8 mL of Dex-NZM (0.5 mg/mL) in 0.1 M NaAc (pH 4.5) or vehicle control (buffer only) for 10 min at room temperature at specific time points (Figure S1). At the end of the experiment (43 h), the Dex-NZM- and vehicle-treated biofilms were placed in 2.8 mL of H_2O_2 (1%, v/v or buffer) for 5 min. After H_2O_2 exposure, the biofilms were washed with sterile saline solution (0.89% NaCl) three times. The biofilms were then removed by a spatula from sHA discs and homogenized *via* bath sonication followed by probe sonication.[12,54,55] Samples of these biofilm suspensions were serially diluted and plated onto blood agar plates using an automated EddyJet Spiral Plater (IUL, SA, Barcelona, Spain). The numbers of viable cells in each biofilm were calculated by counting CFU. The remaining suspension was centrifuged at 5500g for 10 min, the resulting cell pellets were washed twice with water, oven-dried for 2 h, and weighed.[12,55]

Catalytic Activity within Intact Biofilm.—The catalytic activity of 10 kDa Dex-NZM within intact biofilms was measured after incubations similar to those described above. Biofilms grown on sHA disks were treated twice daily by placing them in 2.8 mL of Dex-NZM (0.5 mg/mL) in 0.1 M NaAc (pH 4.5) or vehicle control (buffer only) for 10 min at room temperature at specific time points (Figure S1).[12] At the end of the experimental period (43 h), all the biofilms were washed with 0.1 M NaAc buffer (pH 4.5) three times and transferred to the reaction buffer (500 μL 0.1 M NaAc, pH 4.5 containing 1% H_2O_2 and 100 μg TMB). The reaction was allowed to proceed for 30 min at room temperature without shaking. After the reaction, still images of intact biofilms were acquired, and subsequently, the biofilms were removed using a spatula from the disk surfaces and centrifuged at 5500g for 10 min. Then the absorbance from the supernatant was recorded at 652 nm. Three independent experiments were performed, and the data are presented as mean ± SD.

Distribution of Dex-NZM within Biofilm Architecture.—Confocal fluorescence imaging was performed using an upright microscope (LSM 800, Zeiss) with a 20× (numerical aperture, 1.0) water immersion objective to assess the distribution of Dex-NZM, dynamics of bacterial killing, and EPS degradation within biofilm. Dex-NZM conjugated with Alexa Fluor 488, prepared as described above, was used. SYTO 82 (541/560 nm; Molecular Probes) was used for labeling bacteria, and Alexa Fluor 647-dextran conjugate (647/668 nm; Molecular Probes) was used for labeling insoluble EPS. Each component was illuminated sequentially to minimize cross-talk as follows: Alexa Fluor 488(Dex-NZM) was excited at 488 nm and was collected by a 480/40 nm emission filter; SYTO 82 (bacterial cells) was excited at 560 nm, and was collected by a 560/40 nm emission filter; Alexa Fluor 647 (EPS) was excited at 640 nm and was collected by a 670/40 nm emission filter. To assess colocalization of Dex-NZM with bacteria or EPS, each channel was processed with Otsu's thresholding method using ImageJ. Then, a mathematical function of ImageJ "Process/Image Calculator/And" was applied on thresholded Dex-NZM and bacteria channels (or Dex-NZM and EPS). Finally, the raw integrated densities of each combination were measured.

In addition, we also tested Dex-NZM penetration into the biofilm. Briefly, preformed 19 h *S. mutans* biofilms using UFTYE culture medium (pH 7.0) containing 1% (wt/vol) sucrose at 37 °C were topically treated by placing them in 2.8 mL of Dex-NZM conjugated with Alexa Fluor 488 (0.5 mg/mL) in 0.1 M NaAc (pH 4.5) for 10 min at room temperature. Then the Dex-NZM treated biofilms were placed in 2.8 mL of H_2O_2 (1%, v/v) for 5 min. After H_2O_2 exposure, the biofilms were washed with sterile saline solution (0.89% NaCl), and confocal imaging was performed using a 20× (numerical aperture = 1.0) water immersion objective. SYTO 82 (541/560 nm; Molecular Probes) was used for labeling bacterial cells. Bacteria and Dex-NZM fluorescence images were processed using Otsu's thresholding method. The biofilm thickness was assessed by measuring the height of the microcolonies. Regions of interest (ROI) were set to the center of the microcolony (9 μm^2 size) to assess the penetration of Dex- NZM into the structure, and raw integrated densities of Dex-NZM within ROI were measured. Images were visualized using Amira 5.4.1 software (Visage Imaging, San Diego, CA).

Cell Viability.—The cytotoxicity of each Dex-NZM formulation was evaluated in primary human gingival epithelial cells (HGECs) and human fibroblast (BJ-5ta) cells using the MTS [(3-(4,5-dimethylthiazol-2-yl)-5-(3-carboxymethoxyphenyl)-2-(4-sulfophenyl)-2*H*-tetrazolium)] assay (CellTiter 96 cell proliferation assay kit; Promega, WI, USA).[56] HGECs were a gift from Dr. Manju Benakanakere (School of Dental Medicine, University of Pennsylvania), and BJ-5ta cells were purchased from ATCC (Manassas, VA, USA). HGECs were cultured in keratinocyte serum-free medium (Invitrogen, NY).[57] BJ-5ta cells were cultured in a 4:1 mixture of Dulbecco's Modified Eagle's Medium (DMEM) and medium 199, supplemented with 10% fetal bovine serum (Gibco, NY) and 0.01 mg/mL of hygromycin B (Sigma-Aldrich). The assay was performed in 96-well plates; 10000 cells in 100 μL of cell culture media were added to each well, and then the plates were incubated at 37 °C in a 5% CO_2 atmosphere for 24 h. After this time, the cells were washed gently with sterile phosphate buffered saline (PBS) before 100 μL of Dex-NZM or uncoated NZM (0.5 mg Fe/ml) in cell culture medium was added to the wells. The plates were then incubated at 37 °C in 5% CO2 atmosphere for 10 min. After this incubation, the media was removed, the cells were washed with PBS, and then 20 μL MTS reagent and 100 μL cell culture medium were added to each well. The plates were then incubated at 37 °C in a 5% CO_2 atmosphere for 1 h, after which time the absorbance was recorded at 490 nm using a plate reader. For the 24 h cell viability experiment, the cell culture medium with Dex-NZM was removed from each well after 10 min of incubation. Then the cells were washed with PBS, 100 μL of fresh cell culture medium was added to each well, and the plates incubated for a further 24 h. The MTS reagents were then added and the absorbance was recorded at 490 nm (as described above). Three independent experiments were performed for each Dex-NZM formulation. The percentage of cell viability was calculated and the results were presented as mean ± SD.

Dynamics of Bacterial Killing and EPS Degradation within Intact Biofilm.—For bacterial killing and EPS degradation, SYTO 9 (485/498 nm; Molecular Probes) and propidium iodide (PI, 535/617 nm; Molecular Probes) were used for labeling all and dead cells, and Alexa Fluor 647-dextran conjugate (647/668 nm; Molecular Probes) was used for labeling EPS. The preformed fluorescently labeled biofilm incubated with Dex-NZM was exposed to 1% H_2O_2 (in 0.1 M NaAc buffer at pH 4.5), and time-lapsed confocal imaging was performed in the same field of view at every 20 min (up to 100 min) using a Zeiss LSM 800 upright confocal laser scanning microscope with a 20X (numerical aperture, 1.0) water immersion objective. Each component was illuminated sequentially to minimize cross-talk as follows: SYTO 9 (all bacteria) was excited at 488 nm and collected by a 520/40 nm emission filter; PI (dead bacteria) was excited at 560 nm and was collected by a 600/40 nm emission filter; Alexa Fluor 647 (EPS) was excited at 640 nm and was collected by a 670/40 nm emission filter. Images were analyzed by ImageJ to further quantify the bacterial killing and EPS degradation.

EPS Degradation.—Assessment of EPS degradation was done as described previously.[58] Insoluble EPS glucans were produced by purified *S. mutans*-derived exoenzyme glucosyltransferase B (GtfB) immobilized on a poly-L-lysine-coated MatTek dish and labeled with Alexa Fluor 647-dextran conjugate (Molecular Probes). These fluorescently labeled glucans were then incubated with either vehicle, Dex-NZM (1 mg/mL) alone, 1%

H_2O_2 alone, or Dex-NZM/H_2O2 combination (each in 0.1 M NaOAc buffer at pH 4.5). Time-lapsed confocal imaging was performed in the same field of view every 15 min (up to 90 min), and the images were analyzed with ImageJ.

In Vivo Efficacy of Dex-NZM.—*In vivo* experiments were performed using a rodent model of dental caries.[41,55,59] Briefly, 15 day-old female Sprague—Dawley rat pups were purchased with their dams from Harlan Laboratories (Madison, WI). Upon arrival, animals were screened for *S. mutans* by plating oral swabs on selective media: Mitis Salivarius Agar plus Bacitracin (MSB). Animals that were already infected with *S. mutans* were excluded from the study. The remaining animals were infected by mouth with an actively growing (midlogarithmic) culture of *S. mutans* UA159, and oral swabbing was used to assess the success of this procedure. These animals were given the NIH cariogenic diet 2000 (TestDiet, St. Louis, MO) and 5% sucrose water *ad libitum.* We used a treatment similar to a clinical scenario, which consisted of 1 min topical application of Dex-NZM (at 1 mg/mL) immediately followed by H_2O_2 (at 1%, v/v) exposure (Dex-NZM/H_2O_2). The animals were randomized into four treatment groups, and their teeth were treated twice daily for 21 days. The treatment groups were: (1) control (0.1 M NaAc buffer, pH 4.5), (2) Dex-NZM only (1 mg/mL), (3) 1% H_2O_2 only, and (4) Dex-NZM/ H_2O_2 (1 mg/mL Dex-NZM with 1% H_2O_2). The animals were weighed once a week, and their physical appearances were noted each day. After 21 days of treatment, the animals were sacrificed and their jaws were surgically removed and aseptically dissected. The plaque— biofilm samples were removed and dispersed *via* sonication and subjected to microbiological and microbiome analyses as described previously.[59] All the jaws were defleshed, and the teeth were prepared for caries scoring according to Larson's modification of Keyes' system.[41,60] Determination of caries score of the codified jaws was performed by one calibrated examiner. The gingival and palatal tissues were collected and processed for hematoxylin and eosin (HE) staining for assessment by an oral pathologist (Dr. Faizan Alawi, Penn Oral Pathology).

Statistical Analysis.

At least three independent experiments were performed for each experiment mentioned above. Statistical analysis was carried out using GraphPad Prism 5 software *via* unpaired *t* tests, with the exception of the microbiome data, which were analyzed using *R* (version 3.5.0) with the pairwise Wilcoxon test.

Supplementary Material

Refer to Web version on PubMed Central for supplementary material.

ACKNOWLEDGMENTS

This work was supported by the NIH (R01-DE025848). Additional support was provided by the University of Pennsylvania Research Foundation.

REFERENCES

(1). Koo H; Xiao J; Klein MI; Jeon JG Exopolysaccharides Produced by Streptococcus mutans Glucosyltransferases Modulate the Establishment of Microcolonies within Multispecies Biofilms. J. Bacteriol. 2010, 192, 3024–3032. [PubMed: 20233920]

(2). Flemming HC; Wingender J. The biofilm Matrix. Nat. Rev. Microbiol. 2010, 8, 623–633. [PubMed: 20676145]

(3). Dental Caries (Age 2 to 11). https://www.nidcr.nih.gov/DataStatistics/FindDataByTopic/DentalCaries/DentalCariesChildren2to11.htm (accessed Jan 12, 2019).

(4). Dental Caries and Tooth Loss in Adults in the United States, 2011-2012 https://www.cdc.gov/nchs/products/databriefs/db197.htm (accessed Jan 12, 2019).

(5). Kassebaum NJ; Bernabe E; Dahiya M; Bhandari B; Murray CJ; Marcenes W. Global Burden of Untreated Caries: A Systematic Review and Metaregression. J. Dent. Res. 2015, 94, 650–658. [PubMed: 25740856]

(6). Vos T. Global, Regional, and National Incidence, Prevalence, and Years Lived With Disability for 310 Diseases and Injuries, 1990–2015: A Systematic Analysis for The Global Burden of Disease Study 2015. Lancet 2016, 388, 1545–1602. [PubMed: 27733282]

(7). Beighton D. The Complex Oral Microflora of High-risk Individuals and Groups and its Role in the Caries Process. Community Dent. Oral Epidemiol. 2005, 33, 248–255. [PubMed: 16008631]

(8). Pitts NB; Zero DT; Marsh PD; Ekstrand K; Weintraub JA; Ramos-Gomez F; Tagami J; Twetman S; Tsakos G; Ismail A. Dental Caries. Nat. Rev. Dis. Primers 2017, 3, 17030.

(9). del Pozo JL; Patel R. The Challenge of Treating Biofilm-Associated Bacterial Infections. Clin. Pharmacol. Ther. 2007, 82, 204–209. [PubMed: 17538551]

(10). Koo H; Falsetta ML; Klein MI The Exopolysaccharide Matrix: A Virulence Determinant of Cariogenic Biofilm. J. Dent. Res. 2013, 92, 1065–1073. [PubMed: 24045647]

(11). He Y; Peterson BW; Ren Y; van der Mei HC; Busscher HJ Antimicrobial Penetration in a Dual-Species Oral Biofilm After Noncontact Brushing: An In Vitro Study. Clin. Oral. Investig. 2013, 18, 1103–1109.

(12). Gao L; Liu Y; Kim D; Li Y; Hwang G; Naha PC; Cormode DP; Koo H. Nanocatalysts Promote Streptococcus mutans Biofilm Matrix Degradation and Enhance Bacterial killing to Suppress Dental Caries In Vivo. Biomaterials 2016, 101, 272–284. [PubMed: 27294544]

(13). Hannig M; Hannig C. Nanomaterials in Preventive Dentistry. Nat. Nanotechnol. 2010, 5, 565–569. [PubMed: 20581832]

(14). Hannig M; Hannig C. Nanotechnology and its Role in Caries Therapy. Adv. Dent. Res. 2012, 24, 53–57. [PubMed: 22899680]

(15). Cormode DP; Gao L; Koo H. Emerging Biomedical Applications of Enzyme-Like Catalytic Nanomaterials. Trends Biotechnol 2018, 36, 15–29. [PubMed: 29102240]

(16). Gao L; Koo H. Do Catalytic Nanoparticles Offer an Improved Therapeutic Strategy to Combat Dental Biofilms? Nanomedicine (London, U. K.) 2017, 12, 275–279.

(17). Koo H; Allan RN; Howlin RP; Stoodley P; Hall-Stoodley L. Targeting Microbial Biofilms: Current and Prospective Therapeutic Strategies. Nat. Rev. Microbiol. 2017, 15 (12), 740–755. [PubMed: 28944770]

(18). Besinis A; De Peralta T; Tredwin CJ; Handy RD Review of Nanomaterials in Dentistry: Interactions with the Oral Micro-environment, Clinical Applications, Hazards, and Benefits. ACS Nano 2015, 9, 2255–2289. [PubMed: 25625290]

(19). de Sousa FF; Ferraz C; Rodrigues LK; Nojosa Jde S; Yamauti M. Nanotechnology in Dentistry: Drug Delivery Systems for the Control of Biofilm-Dependent Oral Diseases. Curr. Drug Delivery 2014, 11, 719–728.

(20). Hernandez-Sierra JF; Ruiz F; Pena DC; Martinez- Gutierrez F; Martinez AE; Guillen Ade J; Tapia-Perez H; Castanon GM The Antimicrobial Sensitivity of Streptococcus mutans to Nanoparticles of Silver, Zinc Oxide, and Gold. Nano-medicine 2008, 4, 237–240.

(21). dos Santos VE Jr.; Vasconcelos Filho A; Targino AG; Flores MA; Galembeck A; Caldas AF Jr.; Rosenblatt A. A New “Silver-Bullet” to Treat Caries in Children-Nano Silver Fluoride: A Randomised Clinical Trial. J. Dent. 2014, 42, 945–951. [PubMed: 24930870]

(22). Metin-Gursoy G; Taner L; Akca G. Nanosilver Coated Orthodontic Brackets: In Vivo Antibacterial Properties and Ion Release. Eur. J. Orthod. 2017, 39, 9–16. [PubMed: 26787659]

(23). Ionescu AC; Brambilla E; Travan A; Marsich E; Donati I; Gobbi P; Turco G; Di Lenarda R; Cadenaro M; Paoletti S; Breschi L. Silver-Polysaccharide Antimicrobial Nanocomposite Coating for Methacrylic Surfaces Reduces Streptococcus mutans Biofilm Formation in vitro. J. Dent. 2015, 43, 1483–1490. [PubMed: 26477347]

(24). Allaker RP; Memarzadeh K. Nanoparticles and the Control of Oral Infections. Int. J. Antimicrob. Agents 2014, 43, 95–104. [PubMed: 24388116]

(25). Cormode DP; Sanchez-Gaytan BL; Mieszawska AJ; Fayad ZA; Mulder WJ Inorganic Nanocrystals as Contrast Agents in MRI: Synthesis, Coating and Introducing Multifunctionality. NMR Biomed. 2013, 26, 766–780. [PubMed: 23303729]

(26). van Schooneveld MM; Vucic E; Koole R; Zhou Y; Stocks J; Cormode DP; Tang CY; Gordon R; Nicolay K; Meijerink A; Fayad ZA; Mulder WJM Improved Biocompatibility and Pharmacokinetics of Silica Nanoparticles by Means of a Lipid Coating: a Multimodality Investigation. Nano Lett. 2008, 8, 2517–2525. [PubMed: 18624389]

(27). Gibbons RJ; Banghart SB Synthesis of Extracellular Dextran by Cariogenic Bacteria and its Presence in Human Dental Plaque. Arch. Oral Biol. 1967, 12, 11–23. [PubMed: 4960207]

(28). Xiao J; Klein MI; Falsetta ML; Lu B; Delahunty CM; Yates JR; Heydorn A; Koo H. The Exopolysaccharide Matrix Modulates the Interaction Between 3D Architecture and Virulence of a Mixed- Species Oral Biofilm. PLoS Pathog. 2012, 8, No. e1002623.

(29). Corot C; Robert P; Idee J-M; Port M. Recent Advances in Iron Oxide Nanocrystal Technology for Medical Imaging. Adv. Drug Delivery Rev. 2006, 58, 1471–1504.

(30). Tassa C; Shaw SY; Weissleder R. Dextran-Coated Iron Oxide Nanoparticles: A Versatile Platform for Targeted Molecular Imaging, Molecular Diagnostics, and Therapy. Acc. Chem. Res. 2011, 44, 842–852. [PubMed: 21661727]

(31). Gao L; Zhuang J; Nie L; Zhang J; Zhang Y; Gu N; Wang T; Feng J; Yang D; Perrett S; Yan X. Intrinsic Peroxidase-Like Activity of Ferromagnetic Nanoparticles. Nat. Nanotechnol. 2007, 2, 577–583. [PubMed: 18654371]

(32). Zhang J; Zhuang J; Gao L; Zhang Y; Gu N; Feng J; Yang D; Zhu J; Yan X. Decomposing Phenol by the Hidden Talent of Ferromagnetic Nanoparticles. Chemosphere 2008, 73, 1524–1528. [PubMed: 18804842]

(33). Zhang LH; Zhai YM; Gao N; Wen D; Dong SJ Sensing H_2O_2 with Layer-by-Layer Assembled Fe3O4-PDDA Nano-composite Film. Electrochem. Commun. 2008, 10, 1524–1526.

(34). Unterweger H; Janko C; Schwarz M; Dezsi L; Urbanics R; Matuszak J; Orfi E; Fulop T; Bauerle T; Szebeni J; Journe C; Boccaccini AR; Alexiou C; Lyer S; Cicha I. Non-Immunogenic Dextran-Coated Superparamagnetic Iron Oxide Nanoparticles: A Biocompatible, Size-Tunable Contrast Agent for Magnetic Resonance Imaging. Int. J. Nanomed. 2017, 12, 5223–5238.

(35). Garg B; Bisht T; Ling YC Graphene-Based Nanomaterials as Efficient Peroxidase Mimetic Catalysts for Biosensing Applications: An Overview. Molecules 2015, 20 (8), 14155–90. [PubMed: 26248071]

(36). Naha P; Al-Zaki A; Hecht ER; Chorny M; Chhour P; Blankemeyer E; Yates DM; Witschey WRT; Litt HI; Tsourkas A; Cormode DP Dextran Coated Bismuth-Iron Oxide Nanohybrid Contrast Agents for Computed Tomography and Magnetic Resonance Imaging. J. Mater. Chem. B 2014, 2, 8239–248. [PubMed: 25485115]

(37). Klein MI; Duarte D; Xiao J; Mitra S; Foster TH; Koo H. Structural and Molecular Basis of the Role of Starch and Sucrose in Streptococcus mutans Biofilm Development. Appl. Environ. Microbiol. 2009, 75, 837–841. [PubMed: 19028906]

(38). Xiao J; Klein MI; Falsetta ML; Lu B; Delahunty CM; Yates JR; Heydorn A; Koo H. The Exopolysaccharide Matrix Modulates the Interaction Between 3D Architecture and Virulence of a Mixed- Species Oral Biofilm. PLoS Pathog. 2012, 8, No. e1002623.

(39). Gao LZ; Giglio KM; Nelson JL; Sondermann H; Travis AJ Ferromagnetic Nanoparticles with Peroxidase- Like Activity Enhance the Cleavage of Biological Macromolecules for Biofilm Elimination. Nanoscale 2014, 6, 2588–2593. [PubMed: 24468900]

(40). Chen Z; Wang Z; Ren J; Qu X. Enzyme Mimicry for Combating Bacteria and Biofilms. Acc. Chem. Res. 2018, 51, 789–799. [PubMed: 29489323]

(41). Bowen WH Rodent Model in Caries Research. Odontology 2013, 101, 9–14. [PubMed: 23129523]

(42). van Tilborg GAF; Cormode DP; Jarzyna PA; van der Toorn A; van der Pol SMA; van Bloois L; Fayad ZA; Storm G; Mulder WJM; de Vries HE; Dijkhuizen RM Nanoclusters of Iron Oxide: Effect of Core Composition on Structure, Biocompatibility and Cell Labeling Efficacy. Bioconjugate Chem. 2012, 23, 941–950.

(43). Vasanawala SS; Nguyen K-L; Hope MD; Bridges MD; Hope TA; Reeder SB; Bashir MR Safety and Technique of Ferumoxytol Administration for MRI. Magn. Reson. Med. 2016, 75, 2107–2111. [PubMed: 26890830]

(44). Chiu RYT; Nguyen PT; Wang J; Jue E; Wu BM; Kamei DT Dextran-Coated Gold Nanoprobes for the Concentration and Detection of Protein Biomarkers. Ann. Biomed. Eng. 2014, 42, 2322–2332. [PubMed: 24874602]

(45). Wei H; Wang E. Nanomaterials with Enzyme-Like Characteristics (Nanozymes): Next-Generation Artificial Enzymes. Chem. Soc. Rev. 2013, 42, 6060–6093. [PubMed: 23740388]

(46). Jung CW; Jacobs P. Physical and Chemical Properties of Superparamagnetic Iron Oxide MR Contrast Agents: Ferumoxides, Ferumoxtran, Ferumoxsil. Magn. Reson. Imaging 1995, 13, 661–674. [PubMed: 8569441]

(47). Fattahian Y; Riahi-Madvar A; Mirzaee R; Asadikaram G; Rahbar MR In Silico Locating the Immune-Reactive Segments of Lepidium Draba Peroxidase and Designing a Less Immune-Reactive Enzyme Derivative. Comput. Biol. Chem. 2017, 70, 21–30. [PubMed: 28743101]

(48). Spadiut O; Herwig C. Production and Purification of the Multifunctional Enzyme Horseradish Peroxidase. Pharm. Bioprocess. 2013, 1, 283–295. [PubMed: 24683473]

(49). Bukhari S; Kim D; Liu Y; Karabucak B; Koo H. Novel Endodontic Disinfection Approach Using Catalytic Nanoparticles. J. Endod. 2018, 44, 806–812. [PubMed: 29426645]

(50). Hui JZ; Al Zaki A; Cheng Z; Popik V; Zhang H; Luning Prak ET; Tsourkas A. Facile Method for the Site-Specific, Covalent Attachment of Full-Length IgG onto Nanoparticles. Small 2014, 10, 3354–3363. [PubMed: 24729432]

(51). Hauser AK; Mitov MI; Daley EF; McGarry RC; Anderson KW; Hilt JZ Targeted Iron Oxide Nanoparticles for the Enhancement of Radiation Therapy. Biomaterials 2016, 105, 127–135. [PubMed: 27521615]

(52). Naha PC; Lau KC; Hsu JC; Hajfathalian M; Mian S; Chhour P; Uppulari L; MacDonald ES; Maidment ADA; Cormode DP Gold Silver Alloy Nanoparticles (GSAN): An Imaging Probe for Breast Cancer Screening with Dual-Energy Mammography or Computed Tomography. Nanoscale 2016, 8, 13740–13754. [PubMed: 27412458]

(53). Hayacibara MF; Koo H; Vacca Smith AM; Kopec LK; Scott-Anne K; Cury JA; Bowen WH The Influence of Mutanase and Dextranase on the Production and Structure of Glucans Synthesized by Streptococcal Glucosyltransferases. Carbohydr. Res. 2004, 339, 2127–2137. [PubMed: 15280057]

(54). Falsetta ML; Klein MI; Colonne PM; Scott-Anne K; Gregoire S; Pai CH; Gonzalez-Begne M; Watson G; Krysan DJ; Bowen WH; Koo H. Symbiotic Relationship Between Streptococcus mutans and Candida albicans Synergizes Virulence of Plaque Biofilms in vivo. Infect. Immun. 2014, 82, 1968–1981. [PubMed: 24566629]

(55). Horev B; Klein MI; Hwang G; Li Y; Kim D; Koo H; Benoit DS pH-Activated Nanoparticles for Controlled Topical Delivery of Farnesol to Disrupt Oral Biofilm Virulence. ACS Nano 2015, 9, 2390–2404. [PubMed: 25661192]

(56). Naha PC; Chhour P; Cormode DP Systematic In Vitro Toxicological Screening of Gold Nanoparticles Designed for Nanomedicine Applications. Toxicol. In Vitro 2015, 29, 1445–1453. [PubMed: 26031843]

(57). Guggenheim B; Gmur R; Galicia JC; Stathopoulou PG; Benakanakere MR; Meier A; Thurnheer T; Kinane DF In Vitro Modeling of Host-Parasite Interactions: The 'Subgingival' Biofilm Challenge of Primary Human Epithelial Cells. BMC Microbiol. 2009, 9, 280. [PubMed: 20043840]

(58). Hwang G; Koltisko B; Jin X; Koo H. Nonleachable Imidazolium-Incorporated Composite for Disruption of Bacterial Clustering, Exopolysaccharide-Matrix Assembly, and Enhanced Biofilm Removal. ACS Appl. Mater. Interfaces 2017, 9, 38270–38280. [PubMed: 29020439]

(59). Kim D; Liu Y; Benhamou RI; Sanchez H; Simon-Soro A; Li Y; Hwang G; Fridman M; Andes DR; Koo H. Bacterial- Derived Exopolysaccharides Enhance Antifungal Drug Tolerance in a Cross-Kingdom Oral Biofilm. ISME J. 2018, 12, 1427–1442. [PubMed: 29670217]

(60). Larson RH. Merits and Modifications of Scoring Rat Dental Caries by Keyes' Method; Proc. "Symposium on animal models in cariology"j Spl. Supp. Microbiology Abstracts; 1981. 195–203.

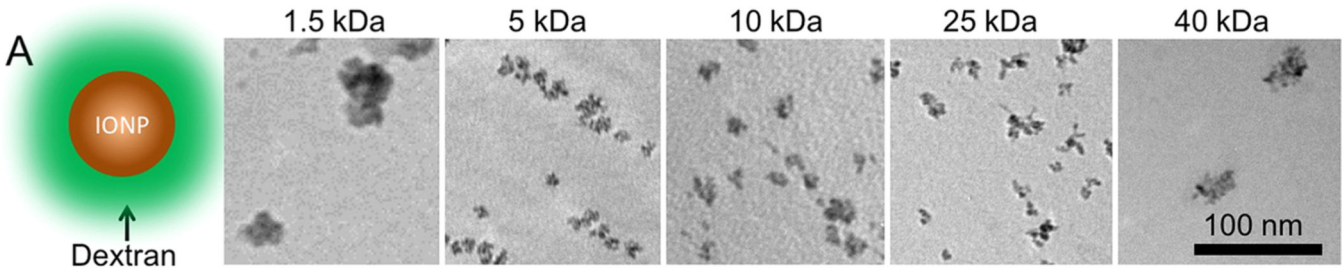

B

Dex-NZM Formulation	Hydrodynamic diameter (nm)	Zeta potential (mV)
1.5 kDa	49 ± 1.2	-17 ± 2
5 kDa	39 ± 0.3	-14 ± 1.7
10 kDa	35 ± 0.2	-18 ± 2
25 kDa	62 ± 1.2	-8.8 ± 1.2
40 kDa	49 ± 0.5	-10 ± 1.3

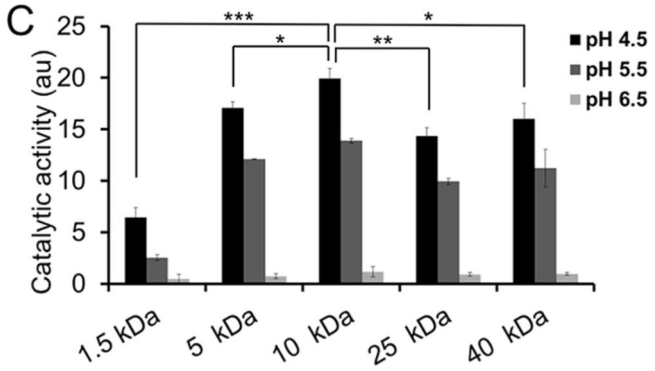

Figure 1.

(A) Schematic and TEM of Dex-NZM formulations (scale bar for all images is the same, *i.e.*, 100 nm). (B) Hydrodynamic diameters and zeta potentials of Dex-NZM measured in DI water. (C) Catalytic activity of different Dex-NZM formulations at three different pHs, as determined from the colorimetric TMB assay. *, **, and *** indicate statistically significant differences of $p < 0.05$, $p < 0.01$, and $p < 0.001$, respectively. Error bars are standard deviations.

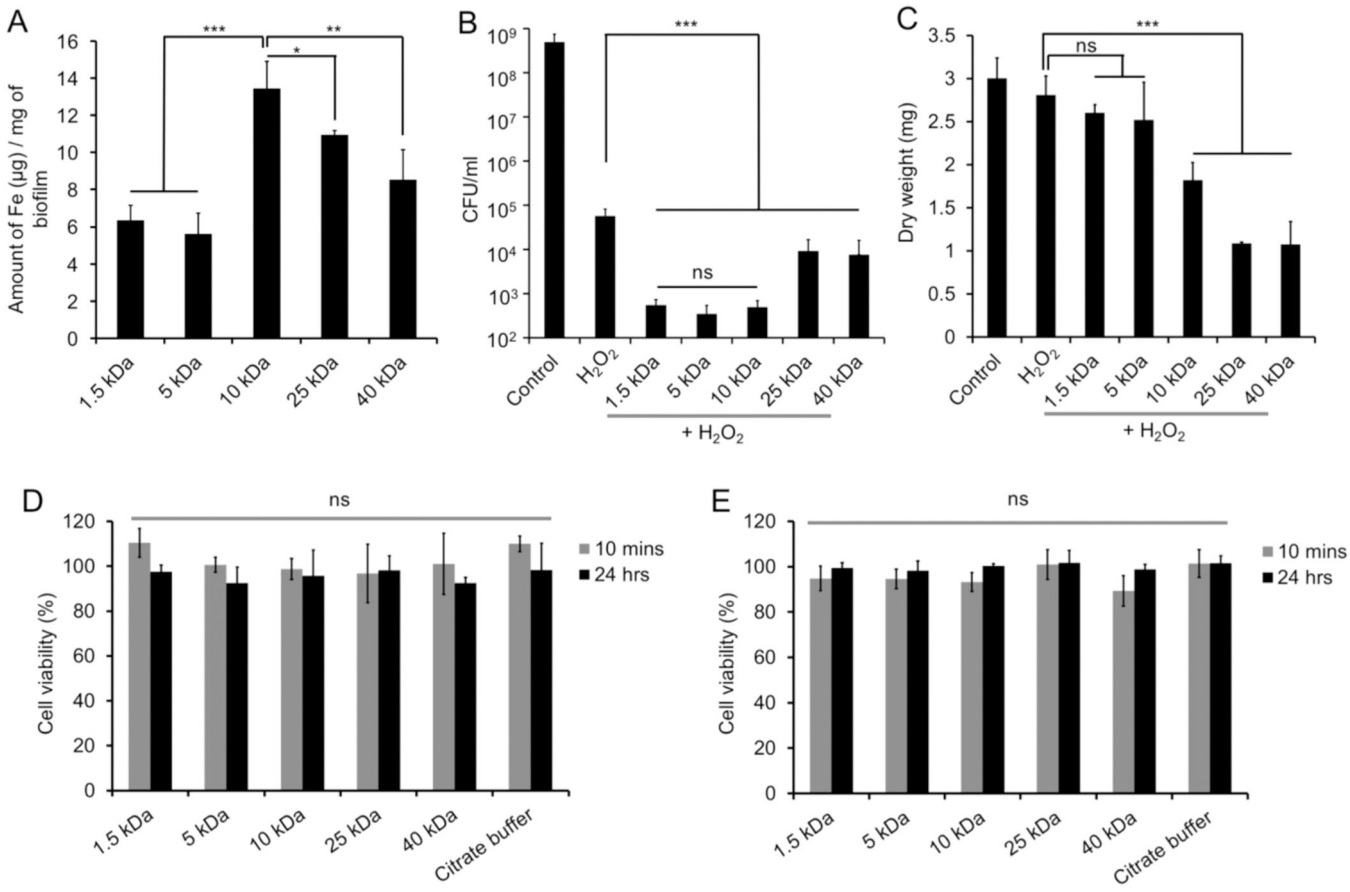

Figure 2.

(A) ICP-OES of biofilm samples (cells and EPS combined) incubated with different Dex-NZM. (B) Effect of different Dex-NZM formulations on bacterial viability with H_2O_2. (C) Effect of Dex-NZM formulations on the mass of biofilms with H_2O_2. Effect of Dex-NZM formulations on the viability of (D) primary human gingival epithelial cells and (E) human fibroblast cells. *, **, and *** indicate statistically significant differences at $p < 0.05$, $p < 0.01$, and $p < 0.001$, respectively, while “ns” stands for nonsignificant difference. Error bars are standard deviations.

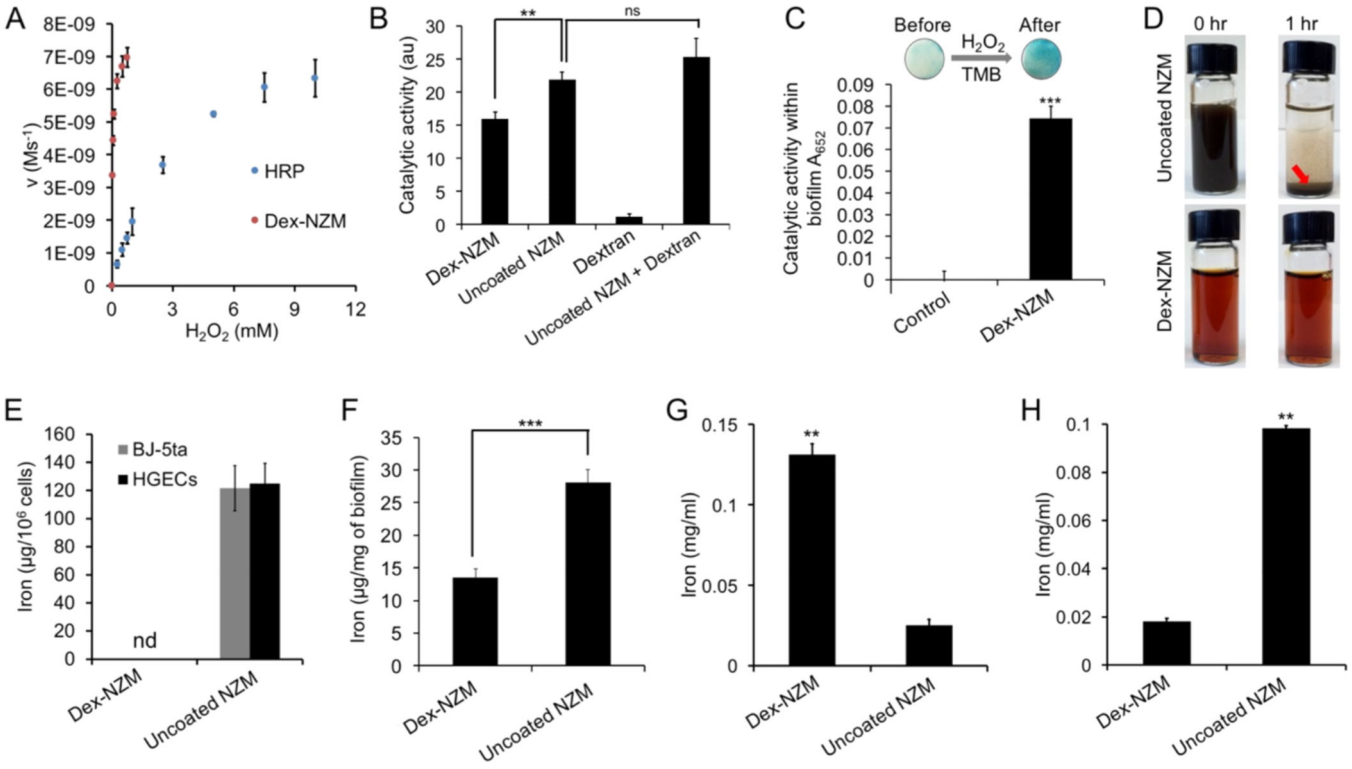

Figure 3.

(A) Reaction kinetics of Dex-NZM and horseradish peroxidase (HRP). (B) Catalytic activity of the formulations noted. (C) Catalytic activity of Dex-NZM within intact biofilms (control is an untreated biofilm). (D) Photographs of uncoated NZM and Dex-NZM in saliva at the time points noted. (E) Binding of NZM to human fibroblasts (BJ-5ta) and human gingival epithelial cells (HGECs). (F) Uptake of NZM in biofilms (incubation concentration: 0.5 mg Fe/mL). (G) Incorporation of NZM in EPS formed by GtfB on hydroxyapatite beads. (H) Binding of NZM to saliva-coated hydroxyapatite beads. ** and *** indicate statistically significant differences from 0 min at $p < 0.01$ and $p < 0.001$, respectively, while “ns” stands for nonsignificant; “nd” stands for nondetected. Error bars are standard deviations.

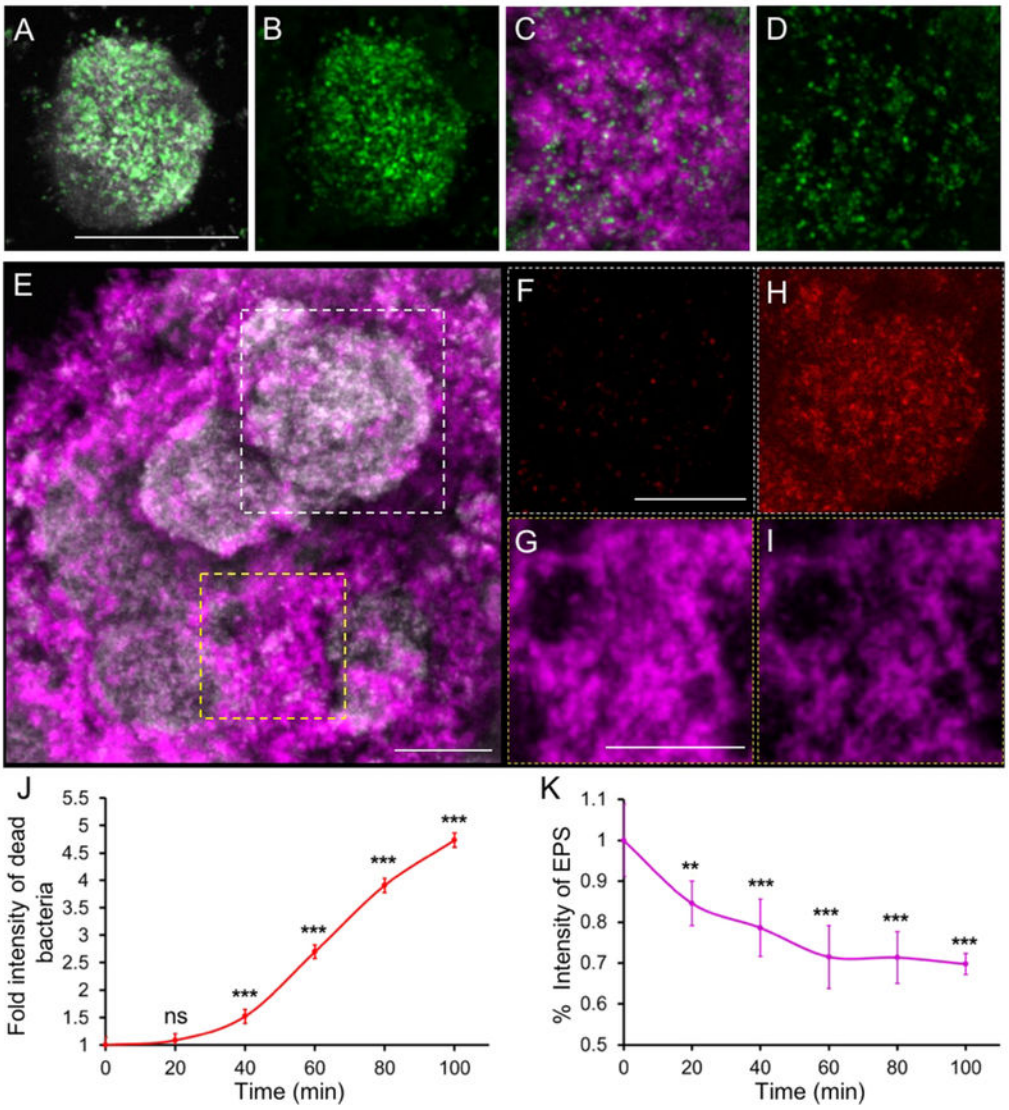

Figure 4.

Antibiofilm properties of topical Dex-NZM + H_2O_2 treatments. (A-D) Distribution of Dex-NZM within a biofilm (gray: bacteria, green: Dex-NZM, magenta: EPS; scale bar: 10 *μm).* (A) Bacterial and Dex-NZM merged image, (B) Dex-NZM image only. (C) EPS and Dex-NZM merged image. (D) Dex-NZM image only. Representative image of a Dex-NZM treated *S. mutans* biofilm (E) before addition of H_2O_2; dashed white and yellow boxed indicate selected areas for localized antibiofilm effects of Dex-NZM. Close-up views of bacteria and EPS images before H_2O_2 exposure (panels F and G, respectively) and 100 min after H_2O_2 exposure (panels H and I). Comparison of (F) and (H) highlights the bacterial killing, while comparison of (G) and (I) indicates EPS-matrix degradation. All bacteria are displayed in gray, and the EPS-matrix is displayed in magenta in (E). Dead bacteria are displayed in red in (F) and (H). The EPS matrix is displayed in magenta in (G) and (I). Scale bar: 50 μm. F—I are higher magnification images from boxed areas in E. (J) Fold intensity of dead bacteria and (K) % intensity of EPS in Dex-NZM treated biofilm over time. ** and

*** indicate statistically significant differences from 0 min at $p < 0.01$ and $p < 0.001$, respectively, while “ns” stands for nonsignificant. Error bars are standard deviations.

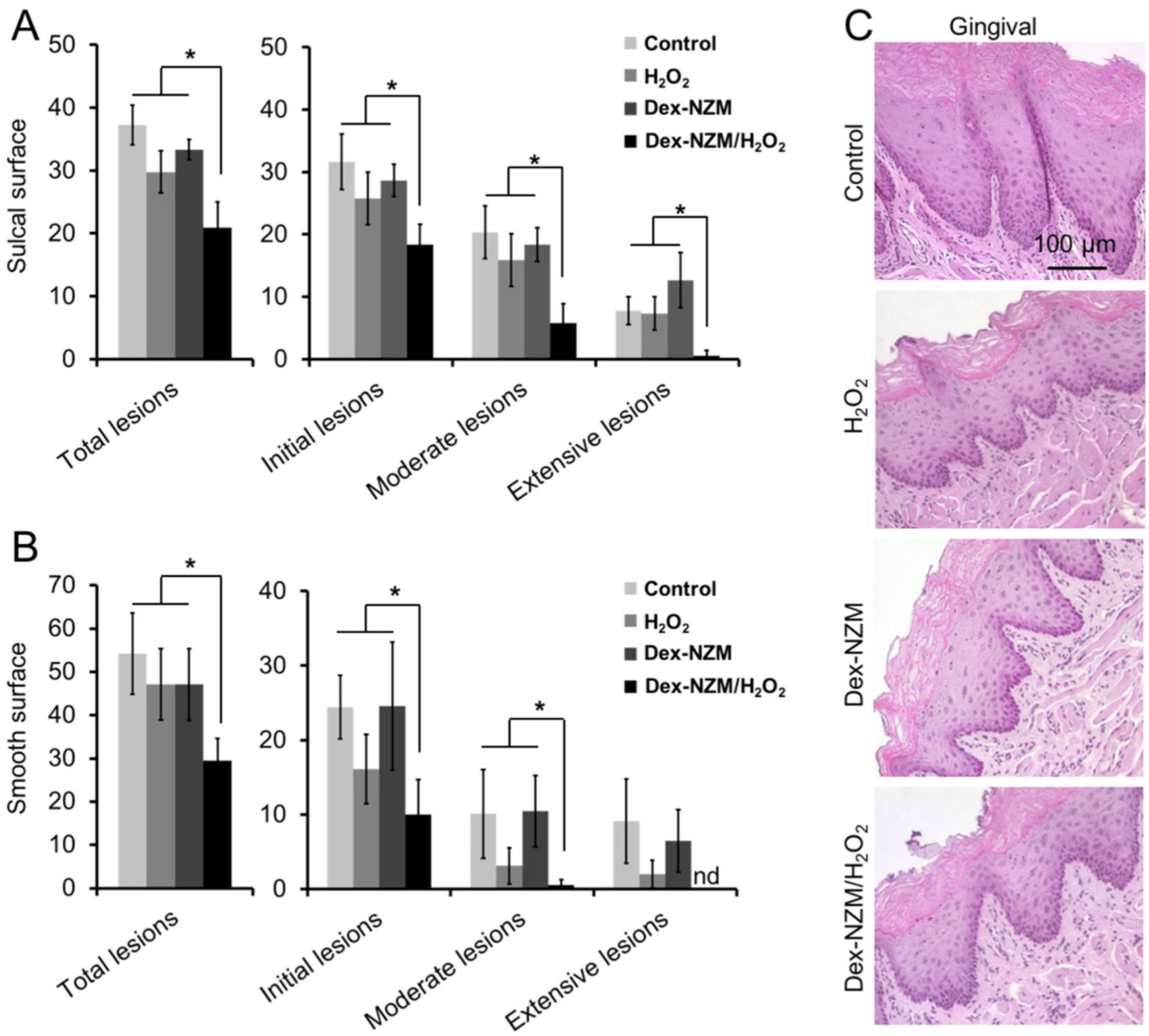

Figure 5.

Effect of Dex-NZM on a biofilm-associated oral disease *in vivo.* (A) Caries scores recorded from sulcal surface. (B) Caries scores recorded from smooth surface. The caries scores were recorded according to Larson's modification of Keyes' scoring system, and the data are presented as mean ± SD ($n = 10$). * indicates significant differences ($p < 0.05$) from control, H_2O_2, or Dex-NZM. (C) Histology of the gingival tissue with the treatments noted. Error bars are standard deviations.